



## Long-time fluctuations of off-diagonal GMI-based magnetometers

Basile Dufay, A. Esper, E. Portalier, C. Dolabdjian, J. Gieraltowski

### ► To cite this version:

Basile Dufay, A. Esper, E. Portalier, C. Dolabdjian, J. Gieraltowski. Long-time fluctuations of off-diagonal GMI-based magnetometers. 2017 IEEE SENSORS, Oct 2017, Glasgow, United Kingdom. 10.1109/ICSENS.2017.8233968 . hal-01708016

HAL Id: hal-01708016

<https://hal.science/hal-01708016>

Submitted on 15 Jun 2018

**HAL** is a multi-disciplinary open access archive for the deposit and dissemination of scientific research documents, whether they are published or not. The documents may come from teaching and research institutions in France or abroad, or from public or private research centers.

L'archive ouverte pluridisciplinaire **HAL**, est destinée au dépôt et à la diffusion de documents scientifiques de niveau recherche, publiés ou non, émanant des établissements d'enseignement et de recherche français ou étrangers, des laboratoires publics ou privés.

# Long-time fluctuations of off-diagonal GMI-based magnetometers

B.Dufay<sup>1</sup>, A. Esper<sup>1</sup>, E. Portalier<sup>1</sup>, C. Dolabdjian<sup>1</sup>, J. Gieraltowski<sup>2</sup>

<sup>1</sup>Normandie Univ, UNICAEN, ENSICAEN, CNRS, GREYC, 14000 Caen, France

<sup>2</sup> LGO/IUEM UMR CNRS 6538, UEB, Université de Bretagne Occidentale,

Place Copernic, Technopôle, Brest-Iroise, 29280 Plouzané, France

basile.dufay@unicaen.fr

**Abstract**—This paper presents the measurement of long-time equivalent magnetic field fluctuations. It was obtained with a low noise off-diagonal GMI magnetometer. Acquisitions are conducted with a dedicated acquisition system. The GMI sensor principle and associated noise sources are reminded. Furthermore, the noise model is extended to include the impact of the very low frequency drift of the associated GMI impedance. The homemade GMI magnetometer and the used high dynamic analog to digital converter board are described. The obtained performances show a peak to peak fluctuations of 10 nT<sub>pp</sub> and a drift of 20 nT/h during 4.5 hours after a transient response. Results are compared, in real time, to a commercial flux gate magnetometer.

**Keywords**—Giant magneto-impedance; magnetometers; noise; long time fluctuations.

## I. INTRODUCTION

The giant magneto-impedance (GMI) effect is based on the large variation of the impedance of a soft magnetic conductor, driven by a high frequency current, when submitted to a change of the external magnetic field applied parallel to the current [1][2]. Since its rediscovery in the 90s [3][4], it has attracted considerable attention due to its potential in high sensitive magnetometry. To develop a highly sensitive magnetometer, attention must be paid on the equivalent magnetic noise level, which describes the undesired fluctuations of the output signal, since it ultimately limits the lowest detectable magnetic field. Usually, equivalent magnetic noise spectral densities of GMI-based devices shows white noise for upper frequency bands (above few kHz), mainly originating from the electronic conditioning circuitry [5]. At lower frequency, an excess noise arises, exhibiting a 1/f behavior, due to intrinsic noise of the sensor related to low frequency fluctuations of the magnetization direction [6].

At even more lower frequency, the characteristics of interest is not the noise power spectral density but the quantification of the long time drift of the output signal. This paper presents preliminary investigation of the long time drift of an optimized GMI-based magnetometer, operating in a field-locked loop.

The paper is organized as follows. Section II recalls the basis of GMI effect, in the context of using it as a sensing element, along with few recalls about noise sources. Section III is dedicated to the description of the experimental setup. Both the electronic conditioning circuitry constituting the magnetometer and the measurement setup are described. Section IV shows the

obtained results which is followed by a general conclusion given in section V.

## II. THEORETICAL BASIS

### A. Principle of the sensing element

The used sensing element is constituted of a CoFeSiB amorphous wire exhibiting GMI effect, strongly coupled to a 450-turns thin pick-up coil. This configuration is usually known as off-diagonal GMI [5] or fundamental mode orthogonal fluxgate [7]. It allows to magnify the intrinsic sensitivity of the device according to the number of turns of the pick-up coil. In the case of a classical setup for off-diagonal configuration, the sine wave excitation current, of amplitude  $I_{ac}$  and frequency  $f_c$ , drives the GMI wire which in turn induces a voltage at the pickup coil ends. This voltage is proportional to the off-diagonal term,  $Z_{21}$ , of the associated impedance matrix and so, reflects its dependence upon external magnetic field. As GMI effect is strongly non-linear versus the applied magnetic field, we usually consider that the sensor operates in a field locked loop. In an open loop, the output signal after demodulation and low-pass filtering,  $V_s$ , has been defined previously [8]. It yields

$$V_s(t) \approx k_d I_{ac} \left[ \left| \frac{\partial Z_{21}(B)}{\partial B} \right|_{B_p} b(t) + z_n(t, T, \dots) \right] + e_n(t) \quad (1)$$

where  $B_p$  is the static field working point of the closed loop,  $b(t)$ , the sensed small signal variation. The term  $\partial Z_{21}/\partial B$  defines the intrinsic sensitivity,  $S_\Omega$ , of the sensing element expressed in  $\Omega/T$  and the factor  $k_d$  is the demodulation gain related to the employed demodulation technique. The terms  $e_n(t)$  and  $z_n(t)$  are the output noise from the electronic conditioning circuitry and the intrinsic noise, respectively. The latter is expressed as an equivalent impedance variation and could depend on external parameters, like the temperature, and could contain terms showing long time drifts. Their corresponding power spectral densities are  $e_n(f)$  and  $z_n(f)$  expressed in  $V/\sqrt{Hz}$  and  $\Omega/\sqrt{Hz}$ , respectively.

### B. Noise Model

As presented in [5], the equivalent magnetic noise level in the white noise region is mainly due to the electronic conditioning circuitry,  $e_n$ . In such a case, the equivalent magnetic noise level is given by the ratio of the output voltage noise to the magnetometer/sensor sensitivity. So that, increasing the sensitivity is usually a way to improve white noise performances.

At lower frequency, the equivalent magnetic noise spectral density exhibits a  $1/f$  behavior. We have recently proposed that the intrinsic fluctuations of the magnetization direction are responsible of this excess noise [6]. These fluctuations could appear in the term  $z_n(t)$  as long as the sensitivity of the GMI impedance to the magnetization direction is known. In our case, the quantity of interest is the equivalent magnetic noise spectral density which relies on the imaginary part of the magnetic susceptibility,  $\chi''$  as previously detailed [6]. It yields

$$b_{n_1/f}^2(f) \approx \frac{3 \mu_0 k_B T}{2\pi f V} \frac{H_{int}^2}{M_s^2} \chi''(f) \quad (2)$$

where  $k_B$  is the boltzmann constant,  $T$  the temperature,  $M_s$  the saturation magnetization of the material,  $H_{int}$  the internal stiffness field, and  $V$  the GMI wire volume. Notice that this model is still valid in locked loop mode as noise performances are not modified by the feedback as long as the feedback field loop is properly done. Furthermore, at even lower frequency, long time fluctuations of the sensing element may affect the output response. Obviously, such fluctuations may also be included in the term  $z_n$  whatever is the physical mechanism responsible of them. Such fluctuations could be due to slow degradations (variations) of the material properties in time or of external influence factors such as the temperature for instance.

### III. EXPERIMENTS

#### A. GMI-based Magnetometer

Measuring long-time fluctuations of a GMI based device requires to use a “true magnetometer” (in the meaning of an instrumentation device) based on a GMI sensing element. This is done when the sensing element is operated in a field locked loop. In such a case, static working point is set and locked by the feedback loop so that the sensing element virtually work in a non-varying magnetic field which is the result of the sum of the external magnetic field to be sensed with the feedback field generated by the feedback loop.

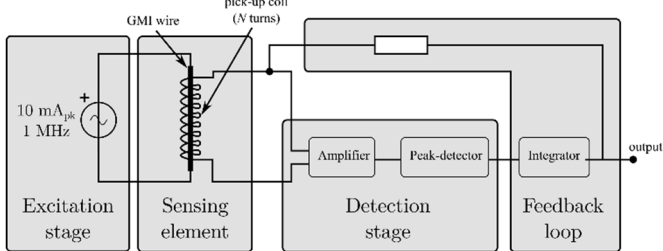


Fig. 1. Block Diagram of the magnetometer.

Overall principle schematic of the magnetometer is given in Fig. 1. It is based on a classic direct chain essentially relying on an excitation stage and a demodulation stage. The first one feeds the GMI wire with a sine wave excitation current of  $10 \text{ mA}_{\text{pk}}$  at an excitation frequency,  $f_c$ , of 1 MHz. Practically, the excitation signal is generated thanks to a direct digital synthesizer (DDS - AD9102), embedded on the magnetometer board. The demodulation stage is made of a diode peak detector, preceded by an amplifier for impedance adaptation regarding the coil impedance at the excitation frequency. The feedback loop incorporates an operational amplifier in pseudo-integrator

configuration insuring that the DC error is removed. It is followed by a resistor and a feedback coil. The latter induces the feedback magnetic field. For integration purpose, the field feedback is done directly through the pick-up coil. The excitation frequency of the sensing element being much higher than the upper limit of the magnetometer band pass ensures correct spectral separation of both signals involved through the pick-up coil. A description of the electronic circuitry is given in [5]. In such setup, noise performances only depend upon those of the direct chain whereas the field feedback sets the linearity range as well as the band pass of the magnetometer. In our case, overall performances of the homemade magnetometer are summarized in Table I.

TABLE I. MAGNETOMETER SPECIFICATIONS

Parameters	Value	Units
Band-pass	300	Hz
Sensitivity	241	kV/T
White noise level	3	pT/ $\sqrt{\text{Hz}}$
Noise level at 1 Hz	100	pT/ $\sqrt{\text{Hz}}$
Dynamic range	$\pm 50$	$\mu\text{T}$

#### B. Measurement setup

Long time fluctuations of the magnetometer are monitored by performing acquisition of the output signal during an important amount of time. In our case, we specifically designed a four-channels data acquisition system based on four 24-bits, low-noise, successive approximation register, analog-to-digital converters (ADC) LTC2380, synchronously clocked at a sampling frequency of 735 kHz. The resulting data flow is preformatted by a programmable logic chip (FPGA Xilinx Artix7), achieving the hard real-time constraints, in order to be transferred to a laptop through USB-3.0 protocol without loss of data. With an averaging factor of 1024, the resulting sampling frequency is 718 Hz, with a corresponding data flow of 11 kB/s on the computer hard disk drive. Further data analyses are then performed on the stored data in differed time by postprocessing. Block diagram of the acquisition system is given in Fig. 2.

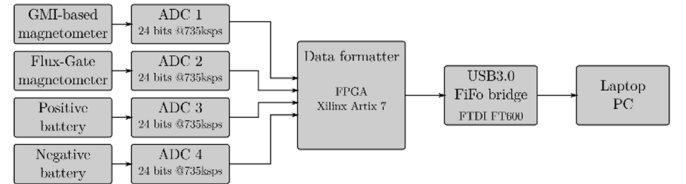


Fig. 2. Block diagram of the acquisition system.

Each ADC is preceded by a low-noise instrumentation amplifier with a programmable gain as to match with several kinds of signals. To validate the setup, the Fig. 3 shows, as an example, the noise power spectral density of our magnetometer obtained from data measured with our acquisition system compared with that obtain thanks to a spectrum analyzer HP3562A (16 bits).

Long time acquisitions are performed in a controlled environment mainly build on a 6-layers magnetic shielded room

placed in a tempered area. Simultaneously, the external magnetic field is measured with a commercial fluxgate magnetometer (*Bartington MAG03*) located near from the GMI magnetometer. Both are battery powered.

#### IV. RESULTS

Acquisition was performed for a duration time longer 4.5 hours. A reference signal was applied at the beginning and at the end of the acquisition sequence to ensure that the overall experimental setup still properly operates.

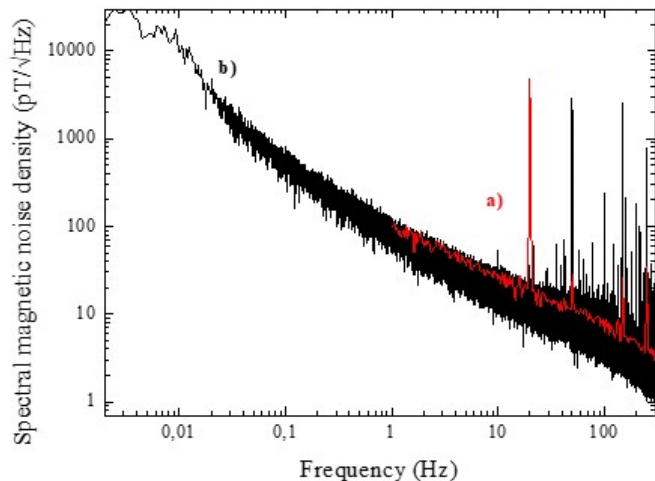


Fig. 3. Equivalent magnetic noise spectral density of the GMI magnetometer. Curve (a) is obtained from spectrum analyzer HP3562A whereas the curve (b) is computed from acquired data with the homemade acquisition system.

During the rest of the acquisition time, no magnetic signal was applied. Temporal plot of the acquired data is given in Fig. 4, expressed in units of magnetic induction (T). One can note that the output signal of the GMI magnetometer shows peak-peak fluctuations of 10 nT during this time period. Variations of the surrounding magnetic field are not involved in these fluctuations as the output of the flux-gate magnetometer doesn't exhibit similar behavior.

#### V. CONCLUSION

A fully embedded GMI-based magnetometer has been designed and characterized. Its performances are fairly comparable to those of its main competitors for low frequency, room temperature, high sensitive magnetometry (particularly fluxgate magnetometers). A dedicated setup has been presented which allows long time acquisition of simultaneous voltage signals with high sampling frequency and dynamic range, suitable for low-noise applications. This setup has been validated against commercial instruments.

Finally, acquisitions of long time fluctuations of GMI-based magnetometer has been performed, showing the relative good performance of GMI-based magnetometer. Remaining fluctuations of the output signal is under investigation. Particularly, the effect of the electronic components drift will be explored as well as physical mechanisms involved in the degradation of the GMI material and the effect of the surrounding temperature variations. Furthermore, longer acquisitions are required, such as weeks or months, to fully qualify this magnetometer compared to the state of the art. This would require specific facilities such as magnetic observatory.

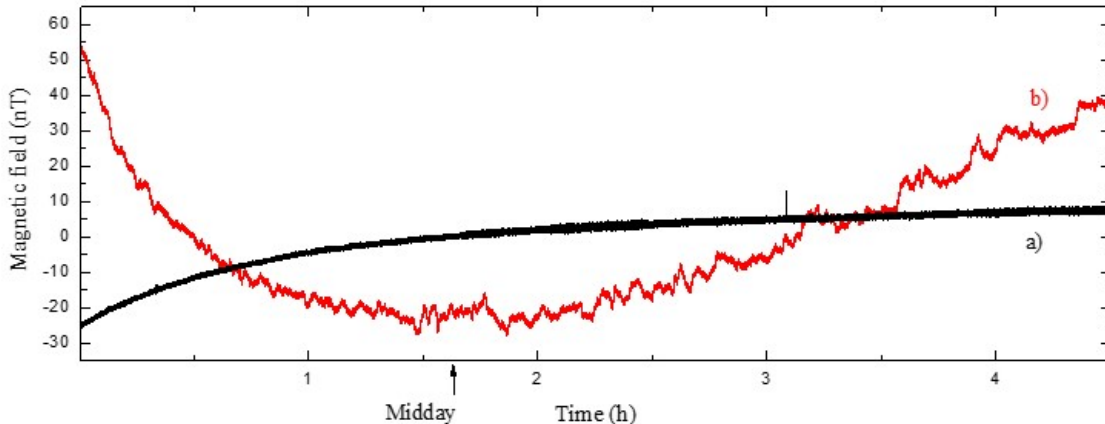


Fig. 4. Long time recording of the magnetometer output signal. Curve (a) and (b) are the GMI-based and fluxgate magnetometer outputs respectively and are expressed in Tesla (T) relying on the left axis.

#### REFERENCES

- [1] M. Knobel, M. Vasquez, and L. Kraus, "Giant magnetoimpedance," *Handbook Magn. Mater.*, vol. 15, pp. 497–563, Dec. 2003.
- [2] M. Phan, and H. Peng, "Giant magnetoimpedance materials: Fundamentals and applications," *Progr. Mater. Sci.*, vol. 53, no. 2, pp. 323–420, Feb. 2008.
- [3] K. Mohri, T. Kohzawa, K. Kawashima, H. Yoshida, and L.V. Panina, "Magneto-inductive effect (MI effect) in amorphous wires," *IEEE Trans. Magn.*, vol. 28, pp. 3150–3152, Sept. 1992.
- [4] R.S. Beach, and A.E. Berkowitz, "Sensitive field- and frequency-dependent impedance spectra of amorphous FeCoSiB wire and ribbon," *J. Appl. Phys.*, vol. 76, pp. 6209–6213, Nov. 1994.
- [5] B. Dufay, S. Saez, C. Dolabdjian, A. Yelon and D. Ménard, "Characterization of an optimized off-diagonal GMI-based magnetometer," *IEEE Sensors J.*, vol. 13, no. 1, Jan. 2013.
- [6] B. Dufay, E. Portalier, S. Saez, C. Dolabdjian, D. Seddaoui, A. Yelon, and D. Ménard, "Low frequency excess noise source investigation of off-diagonal GMI-based magnetometers," *IEEE Trans. Magn.*, vol. 53, no. 1, Jan. 2017.
- [7] E. Paperno, "Suppression of magnetic noise in the fundamental-mode orthogonal fluxgate," *Sensors Actuat. A, Phys.*, vol. 116, no. 3, pp. 405–409, 2004.
- [8] E. Portalier, B. Dufay, S. Saez, and C. Dolabdjian, "Noise behavior of high sensitive GMI-based magnetometer relative to conditioning parameters," *IEEE Trans. Magn.*, vol. 51, no. 1, p. 4002104, Jan. 2015.